

Microwave adsorption of core–shell structure polyaniline/SrFe₁₂O₁₉ composites

C. L. Yuan · Y. S. Hong

Received: 5 August 2009 / Accepted: 2 March 2010 / Published online: 14 March 2010
© Springer Science+Business Media, LLC 2010

Abstract Polyaniline/strontium hexaferites (PANI/SrFe₁₂O₁₉) composites were synthesized by the oxidative chemical polymerization of aniline in the presence of APS. X-ray powder diffraction of ferrites indicated that the structure of core materials is hexagonal with lattice constants around 5.886–5.885 Å. The structural in the character of the sol–gel was investigated with Fourier transform infrared spectrometer analysis. SEM and TEM photographs show that the particle size of core material is around 50–200 nm. After coating with polyaniline, the particle size of the core–shell of PANI/SrFe₁₂O₁₉ has grown up to 100~300 nm. In the magnetization for the PANI/SrFe₁₂O₁₉ composites, it was found that the saturation magnetization (M_s) and coercivity (H_c) decreased after polyaniline coating. The composite under applied magnetic field exhibited the hysteretic loops of the ferromagnetic behavior, such as high saturation magnetization ($M_s = 18.9$ emu/g) and coercivity ($H_c = 3850.0$ Oe). The conductivity of the core–shell materials increased with increasing amounts of polyaniline as the temperature increased from 0 to 50 °C, the conductivity increased by about 13%. The polymerization mechanism for the core–shell composites was also investigated. The composite specimens of core–shell PANI/SrFe₁₂O₁₉ and thermal plastic resin (TPR) had band-width microwave absorption due to reflection losses from –27.3 to –37.4 dB at frequencies between 10.5 and 11.8 GHz as observed by High-frequency network analyzer.

C. L. Yuan (✉)
Department of Chemistry, R. O. C. Military Academy, No. 1,
Fengshon, Kaohsiung 830, Taiwan, ROC
e-mail: junelong@mail2000.com.tw

Y. S. Hong
Department of Applied Chemistry and Material Science, Chung
Cheng Institute of Technology, NDU, No. 190, Sanyuan 1st St.
Dahsi, Jen, Taoyuan, Taiwan, ROC

Introduction

In recent decades, conducting polymers have attracted much attention because of their potential applications in various fields such as molecular electronic, antistatic coatings, electromagnetic interference (EMI) shielding, rechargeable batteries, chemical sensor, corrosion inhibitors, microwave absorbing materials [1–5], etc. Among the conducting polymers, polyaniline (PANI) has been extensively studied due to its easy synthesis, low cost, excellent environmental stability, and high electrical conductivity [6, 7]. It is well known that conducting polymers can effectively shield electromagnetic waves generated by an electric source, whereas electromagnetic waves from a magnetic source can be effectively shielded only by magnetic materials [8, 9]. Thus, incorporation of magnetic constituents and conducting polymeric materials opens new possibilities for the achievement of good shielding for various electromagnetic sources.

M-type strontium hexaferites SrFe₁₂O₁₉ (SrM) is currently a magnetic material with great scientific and technological interest, and has been widely used for permanent magnets, magnetic recording media, and microwave absorbers, due to its high stability, excellent high-frequency response, large magneto-crystalline anisotropy, and large magnetization as well [10]. In recent years, M-type hexagonal ferrite has displayed a promising application in microwave absorption due to their permittivity and permeability losses in the microwave frequency band [11]. Up to now, many reports have focused on choosing the hexaferrite as the magnetic component in polyaniline-based composites, as in [12–14]. To our knowledge, there have not been any other reports on detailed studies related to modifying the magnetic properties of conducting polyaniline coating and strontium hexaferrite composites (PANI/SrM) with our method.

In this article, electromagnetic functionalized polyaniline/SrFe₁₂O₁₉ composites, where the SrFe₁₂O₁₉ particles were magnetic cores obtained using the aqueous combustion synthesis (ACS) method in the glycine–metal nitrate sol–gel system and polyaniline (PANI) was the conducting shell, were synthesized by the oxidative chemical polymerization of aniline in the presence of ammonium peroxydisulfate (APS). A possible polymerization mechanism for PANI/SrFe₁₂O₁₉ composites is also discussed. The samples were characterized by various experimental techniques, and the conductivity of PANI/SrFe₁₂O₁₉ at three different temperatures was measured, and the magnetization properties of the composites were investigated. The absorption of microwaves and the relative complex permittivity and permeability of the composite powders were also investigated.

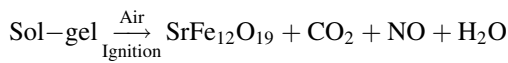
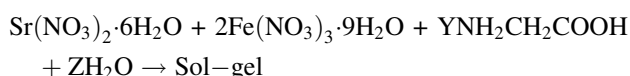
Experimental

Materials

Aniline was distilled twice under reduced pressure and stored below 0 °C. Citric acid, ammonia, HCl, Fe(NO₃)₃·9H₂O, Sr(NO₃)₂ and (NH₄)₂S₂O₈ (ammonium peroxydisulfate, APS) were all of analytical purity and used without further purification.

Preparation of SrFe₁₂O₁₉ hexaferrite (SF) particles

Stoichiometric amount of metal nitrates were dissolved completely in 100 mL of deionized water to form aqueous solution I. Aqueous solution II was prepared by dissolving the proper amount of glycine in deionized water. Solution I and solution II were mixed and the resulting solution was heated in an oil-bath at 120 °C for 4 h to evaporate part of the water until high viscosity wet gels were formed. Afterward, the wet gel was ignited in air. Self-propagation using ACS in a glycine–metal nitrate system, and deep gray and voluminous as-burnt powders were obtained. The combustion reaction of the gels can be described simply as follows:



The as-burnt powders were the precursors of hexagonal ferrite SrFe₁₂O₁₉. Finally, the expected nano-particles size of the hexaferrite powders were obtained by annealing the as-burnt powers at 1200 °C for 2 h.

Preparation of PANI/SrFe₁₂O₁₉ composites

The core–shell materials of PANI/SrFe₁₂O₁₉ were prepared by the oxidative chemical polymerization of aniline on the surface of ferrite, which were suspended in an aqueous solution containing the oxidative agent HCl. In order to improve the contacts between the ferrites and anilines in the aqueous solution, nano-sized ferrites were dispersed in deionized water by ultrasonic waves for 30 min before polymerization, and 2.49 g APS in 0.1 M HCl was added to the aqueous solution at the same time. Then the required amount of aniline was placed in the flask, and the polymerization was allowed to proceed at a temperature between 0 and 5 °C under stirring for 10 h. After the solid core–shell particles were formed, the solid products were collected and washed with methanol and deionized water several times. Finally, the products were dried in a vacuum oven at 100 °C for 24 h.

Characterization

The XRD patterns of the samples were collected using powder X-ray diffraction (XRD) (Siemens D5000X) with Cu K α radiation ($\lambda = 0.15418$ nm). Fourier transmission infrared (FTIR) spectra were recorded on a Brucker VECTOR22 spectrometer from Varian) in the range of 500–4000 cm⁻¹ using KBr pellets. The morphology was characterized by a JSM-6390 scanning electron microscope (SEM) and JEOL2000-EX 2 transmission electron microscope (TEM). Magnetic measurements were carried out at room temperature using a vibrating sample magnetometer (VSM, Lake Shore, Model 7400) with a maximum magnetic field of 15 kOe. The conductivity of samples at different temperature (0, 25, and 50 °C) was determined with a Keithley 2410 DC voltage–current detector. The specimens for microwave adsorption testing were prepared by homogeneously mixing the composite powders with 25 wt% thermal plastic resin (TPR). High-frequency network analyzer (HP 8510C) was used to measure the reflection loss (RL) of electromagnetic radiation of the SrFe₁₂O₁₉–TPR, PANI/SrFe₁₂O₁₉–TPR composite materials, respectively. The reflection loss curves were calculated from the complex relative permeability and permittivity at a given frequency and absorber thickness with the following equations:

$$Z_{in} = \sqrt{\frac{\mu_r}{\epsilon_r}} \tan h \left[\left(j \frac{2\pi}{\lambda} \right) d \sqrt{\mu_r \epsilon_r} \right] \quad (1)$$

$$\Gamma = \frac{Z_{in} - 1}{Z_{in} + 1} \quad (2)$$

$$RL(\text{dB}) = 20 \times \log |\Gamma| \quad (3)$$

where λ is the frequency, d the thickness of the absorber, c the velocity of light, ε_γ and μ_γ are the relative complex permeability and permittivity of the absorber medium, Γ is the reflection parameter, Z_0 the impedance of air and Z_{in} the input impedance of the absorber [15].

Results and discussions

X-ray powder diffraction

The XRD patterns of $\text{SrFe}_{12}\text{O}_{19}$, PANI/ $\text{SrFe}_{12}\text{O}_{19}$ composite nano-particles and PANI are shown in Fig. 1. As shown in Fig. 1c, the crystal structures of $\text{SrFe}_{12}\text{O}_{19}$ annealed at 1200 °C for 2 h were determined by the powder X-ray diffraction technique. The X-ray diffraction patterns of $\text{SrFe}_{12}\text{O}_{19}$ particles present the M-type structure, and the XRD spectra showed the diffraction peaks of hexagonal $\text{SrFe}_{12}\text{O}_{19}$ (110), (107), (114), (203), (205), (206), (0014), (304), (221), and (404), which were all observed in each curve [16]. The lattice constants a of $\text{SrFe}_{12}\text{O}_{19}$ is 5.886–5.885 Å. A typical XRD pattern of polyaniline shows one broad diffraction peak centered at $2\theta = 25.51^\circ$ (see Fig. 1a), which can be ascribed to the periodicity parallel and perpendicular to the polymer chains [17]. Figure 1b shows the values of the PANI/ $\text{SrFe}_{12}\text{O}_{19}$ composite, which contains the characteristic peaks of PANI and $\text{SrFe}_{12}\text{O}_{19}$ including the peaks at $2\theta = 25.51^\circ$, 30.39°, 32.28°, 34.03°, 50.30°, 56.17° and 76.19°, respectively. These results indicated that the structure of core materials is hexagonal and PANI/ $\text{SrFe}_{12}\text{O}_{19}$ that the core–shell composite were obtained.

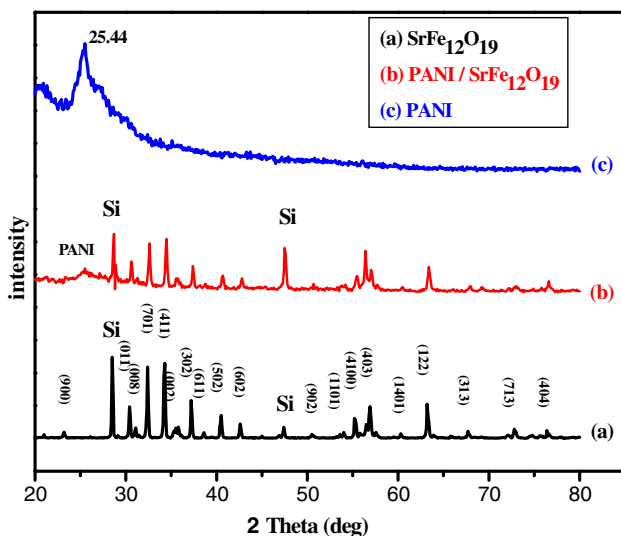


Fig. 1 XRD patterns of (a) $\text{SrFe}_{12}\text{O}_{19}$ particles, (b) PANI/ $\text{SrFe}_{12}\text{O}_{19}$ composite, and (c) PANI

FTIR spectral analysis

The FTIR spectra of the strontium hexaferrites, PANI/ $\text{SrFe}_{12}\text{O}_{19}$ composites, and PANI sample without $\text{SrFe}_{12}\text{O}_{19}$ core-particles under the same conditions are shown in Fig. 2. It is observed in Fig. 2b that there is the peak at 500–600 cm⁻¹ (corresponding to vibrations of the octahedral and tetrahedral sites for $\text{SrFe}_{12}\text{O}_{19}$) in each curve. The characteristic peaks of PANI occur at 1115, 1237, 1296, 1488, 1557, and 805 cm⁻¹. The peaks at 1557 and 1488 cm⁻¹ are attributed to the characteristic C=C stretching of the quinoid and benzenoid rings, and the peaks at 1296 and 1237 cm⁻¹ correspond to N–H bending and asymmetric C–N stretching modes of the benzenoid ring, which were also observed in each curve of Fig. 2a. The peak around 1115 cm⁻¹ is associated with vibrational modes of N=Q=N (Q refers to the quinonic-type rings), indicating that PANI was formed in our sample. The peak at 805 cm⁻¹ was attributed to the out-of-plane deformation vibration of the *p*-disubstituted benzene ring. The absorption peaks of the PANI/ $\text{SrFe}_{12}\text{O}_{19}$ composite shifted to 1573 and 1,136 cm⁻¹ (see Fig. 2c). The absorption peak of the composite with PANI/ $\text{SrFe}_{12}\text{O}_{19}$ is about 16 and 21 cm⁻¹ shifted compared to that of the pure PANI. These results indicate the good quality of the coating of $\text{SrFe}_{12}\text{O}_{19}$ particle with PANI in the composite.

SEM and TEM observation

From the SEM micrograph, diameter of the hexagonal $\text{SrFe}_{12}\text{O}_{19}$ powders were found to increase, distributed in the range of 50–200 nm (Fig. 3a) after heat treatment at 1200 °C for 2 h. Figure 3b shows the SEM image of the core–shell PANI/ $\text{SrFe}_{10}\text{O}_{19}$. The image indicates that the

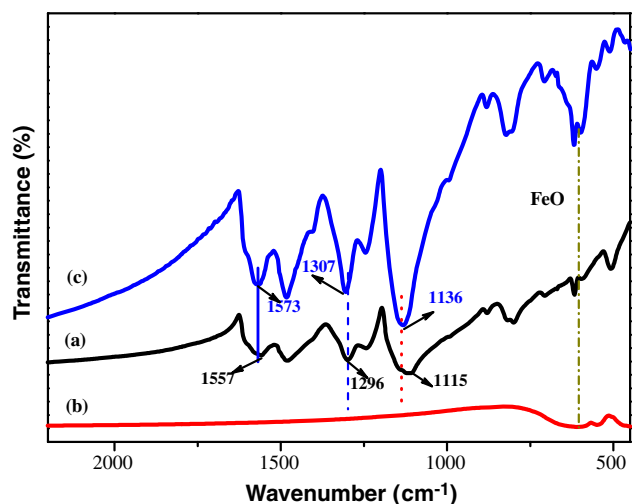


Fig. 2 FT-IR spectra of prepared with different PANI/ $\text{SrFe}_{12}\text{O}_{19}$ (a) PANI; (b) $\text{SrFe}_{12}\text{O}_{19}$; (c) PANI/ $\text{SrFe}_{12}\text{O}_{19}$ composite

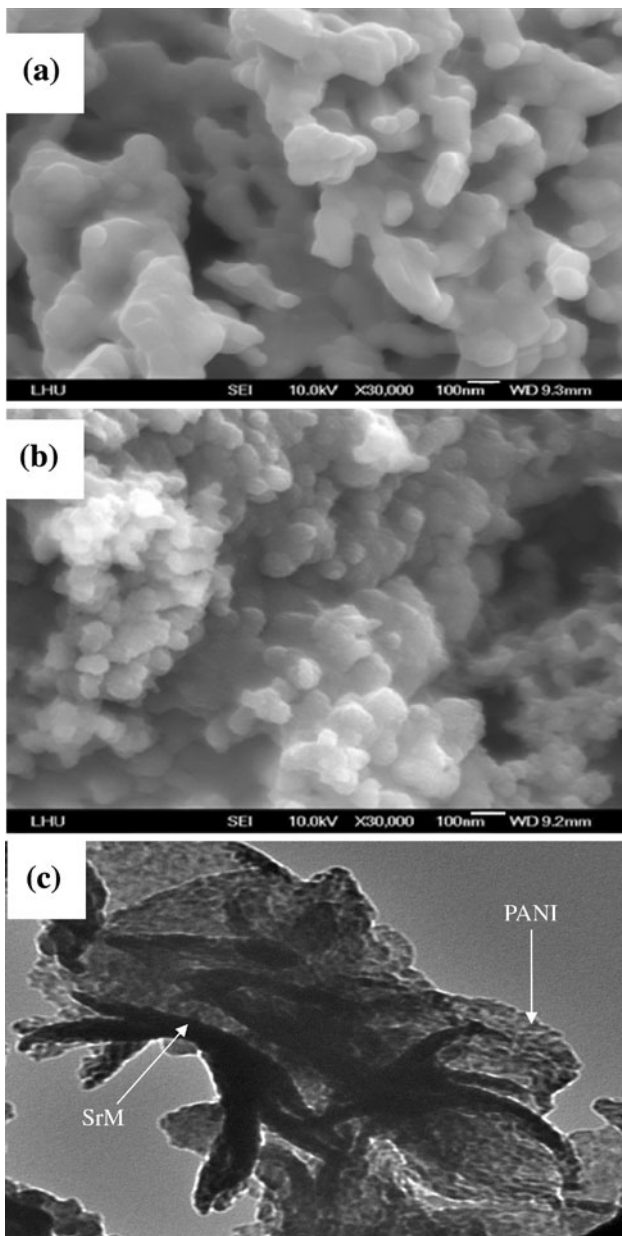


Fig. 3 SEM images of **a** $\text{SrFe}_{12}\text{O}_{19}$ particles, **b** PANI/ $\text{SrFe}_{12}\text{O}_{19}$ composites. TEM images of **c** PANI/ $\text{SrFe}_{12}\text{O}_{19}$ composite

core–shell are coated by polyaniline and form spherical coral-like particles, which have diameters around 100–300 nm and are connected by polymer. To investigate the detailed structure of PANI/ $\text{SrFe}_{10}\text{O}_{19}$ core–shell samples, TEM was performed. The PANI/ $\text{SrFe}_{10}\text{O}_{19}$ powder composite was dissolved with *N*-methyl-2-pyrrolidone (NMP), which is a good dissociation solvent for PANI. Figure 3c shows the $\text{SrFe}_{10}\text{O}_{19}$ particles coated by PANI layer, and indicate that the $\text{SrFe}_{10}\text{O}_{19}$ particles are embedded in the PANI matrix. The black region is $\text{SrFe}_{10}\text{O}_{19}$ particles, and the gray colored shell is PANI in the composite, due to the different electron penetrability.

Magnetic properties

Figure 4 shows the hysteresis loops of the $\text{SrFe}_{12}\text{O}_{19}$ particles, PANI/ $\text{SrFe}_{12}\text{O}_{19}$ composites, and pure PANI at room temperature. It is observed in Fig. 4a, the saturation magnetization (M_s), coercivity (H_c), and remanence magnetization (M_r) values for $\text{SrFe}_{12}\text{O}_{19}$ are $M_s = 57.7 \text{ emu/g}$, $H_c = 3553.0 \text{ Oe}$, and $M_r = 32.9 \text{ emu/g}$, respectively. In contrast, the PANI/ $\text{SrFe}_{12}\text{O}_{19}$ composites under applied magnetic field exhibit a clear hysteretic behavior. As seen from Fig. 4b, c, the $M_s = 37.3, 18.9 \text{ emu/g}$, and $H_c = 2969.7, 3850.0 \text{ Oe}$ for 25.5 and 42.0 wt% PANI/ $\text{SrFe}_{12}\text{O}_{19}$ composites are lower than those of pure $\text{SrFe}_{12}\text{O}_{19}$ particles, respectively. Figure 4d shows the pure PANI magnetic properties are $M_s = 5.3 \text{ emu/g}$ and $H_c = 1915.1 \text{ Oe}$, respectively. When PANI = 25.5–42.0 wt% (Fig. 4b, c.), the values of H_c , M_s , and M_r all decreased with increasing PANI values, and contraction of the hysteresis loop area is seen. These result shows that the $\text{SrFe}_{12}\text{O}_{19}$ cores are responsible for the magnetic behavior of the PANI/ $\text{SrFe}_{12}\text{O}_{19}$ composites. According to the equation $M_s = \varphi m_s$, M_s is related to the volume fraction of the particles (φ) and the saturation moment of a single particle (m_s) [18]. It can be assumed that the M_s of the PANI/ $\text{SrFe}_{12}\text{O}_{19}$ composite depends mainly on the volume fraction of the magnetic hexaferrite particles, due to the contribution of the non-magnetic PANI coating layer to the total magnetization, resulting in a decrease in the saturation magnetization. The magnetic properties observed for magnetic particles are a combination of many anisotropy mechanisms. An effective anisotropy constant (K) could be obtained by adding the bulk anisotropy and surface contributions, and the following expression has been used to account for K [19]:

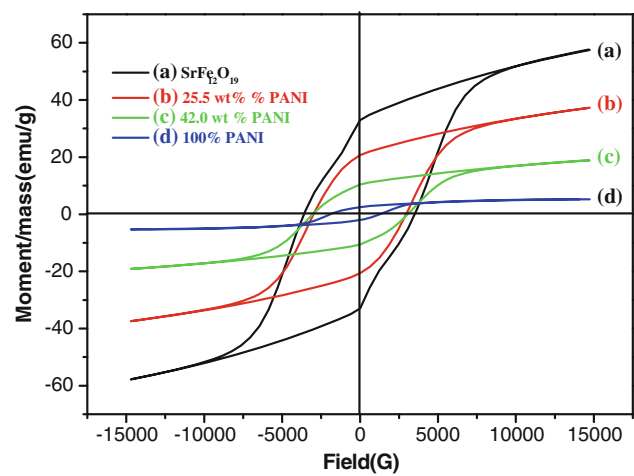


Fig. 4 Hysteresis loops of $\text{SrFe}_{12}\text{O}_{19}$ particles, PANI/ $\text{SrFe}_{12}\text{O}_{19}$ composites and pure PANI

$$K = K_b + (6/d)K_s \quad (4)$$

where K_b is the bulk magnetocrystalline anisotropy, K_s is the surface anisotropy and d is the particle diameter. K_s is usually maximum for free surfaces and is reduced by solid coverage. The decrease in K_s resulting from the particle coverage by the PANI reduces the effective magnetocrystalline anisotropy (K) and therefore decreases H_c .

Resistivity

The resistivities of polyaniline (PANI), $\text{SrFe}_{12}\text{O}_{19}$, and the core–shell materials of PANI/ $\text{SrFe}_{12}\text{O}_{19}$ were measured using a Keithley 2410 DC voltage–current detector. The data on the resistivity of the materials are shown in Table 1 and Fig. 5. Based on the results, the reactivities of all hexagonal ferrites are on the order of $10^4\text{--}10^5 \Omega \text{ cm}$, which are the conductivities of metallic oxides or ferrites at room temperature. In this work, pure PANI has a resistivity of only $0.61 \Omega \text{ cm}$ (a conductivity of 1.64 S cm^{-1}), which is less than the resistivity of PANI according to an earlier work, $0.85 \Omega \text{ cm}$ (a conductivity of 1.17 S cm^{-1}) [12]. The temperature relationship of the conductivity of the core–shell materials and the amount of PANI in core–shell materials is shown in Fig. 5. Figure 5 indicates that the values of $\log \rho^{-1}$ (ρ is the resistivity) of core–shell PANI/ $\text{SrFe}_{12}\text{O}_{19}$ materials increase dramatically with increasing PANI in the materials, and conductivities as high as $10^{-1} \Omega^{-1} \text{ cm}^{-1}$ in the core shell Sr–Fe ferrite–PANI, containing about 71%, can be obtained. When the temperature increased from 0 to 25 °C and 50 °C, the conductivity increased by about 13%. Thus, the PANI mass ratio and temperature both influence conductivity.

Polymerization mechanism of PANI/ $\text{SrFe}_{12}\text{O}_{19}$ composites

The polymerization mechanism of core–shell composites that are composed of hexaferrites and polyaniline is proposed. The aniline monomers were polymerized in the presence of APS. It is known that the polymerization

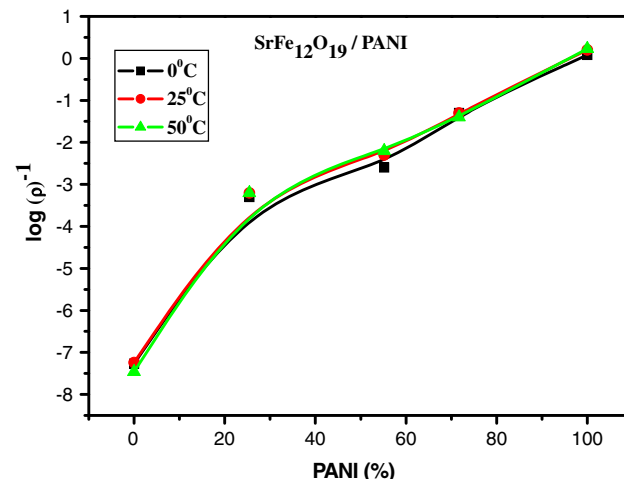


Fig. 5 Effect of PANI content in the composites on the $\log \rho^{-1}$ of core–shell PANI/ $\text{SrFe}_{12}\text{O}_{19}$ materials. ρ is the resistivity of material

location of the polyaniline monomer can be divided into two places [16]. The charge compensation mechanism indicates that there is a charge compensation effect between the hexaferrites and PANI chains in the composites. The surface of the ferrite is positively charged due to the polymerization in acidic conditions. Therefore, adsorption of an amount of chloride anions (Cl^-) may compensate for the positive charges on the ferrite surface. Moreover, in this charge compensation system, extra adsorption of the Cl^- on the ferrite surface would work as the charge compensator for positively charged PANI chains in the formation of PANI/ $\text{SrFe}_{12}\text{O}_{19}$ composites. It is also probable that there is hydrogen bonding between the polyaniline chains and the oxygen atoms on the ferrite surface in the core–shell composites, which causes the ferrite particles to be embedded into the polymer chains of PANI. The σ – π interaction between hexaferrites and PANI may also occur in the composites, which includes two mechanisms: one involves the π molecular orbital of PANI overlapping the empty d -orbital of Fe^{3+} ions to form a σ -bond, where the metallic empty d -orbital is the electron pair acceptor, and the other involves the π^* molecular orbital of PANI overlapping the d -orbital of Fe^{3+} to form a

Table 1 Conductivity of core–shell PANI/ $\text{SrFe}_{12}\text{O}_{19}$ at different temperatures

Temp.	0 °C		25 °C		50 °C	
	$\sigma (\text{S cm}^{-1})$	$\rho (\Omega \text{ Cm})$	$\sigma (\text{S cm}^{-1})$	$\rho (\Omega \text{ Cm})$	$\sigma (\text{S cm}^{-1})$	$\rho (\Omega \text{ Cm})$
0	1.60×10^{-6}	625,704	1.72×10^{-5}	58,197	1.03×10^{-5}	97,219
25.45	4.8×10^{-4}	2.1×10^{-3}	6.7×10^{-4}	1.5×10^{-3}	5.9×10^{-4}	1.7×10^{-3}
55.16	2.60×10^{-3}	390	5.00×10^{-3}	210	3.10×10^{-3}	320
56.59	4.50×10^{-2}	22	4.50×10^{-2}	22	4.00×10^{-2}	25
71.7	1.1	0.92	1.5	0.68	0.91	1.1
100	1.20	0.86	1.64	0.61	1.71	0.585

Fig. 6 The simple synthesis procedure mechanism of core-shell materials of PANI/SrFe₁₂O₁₉

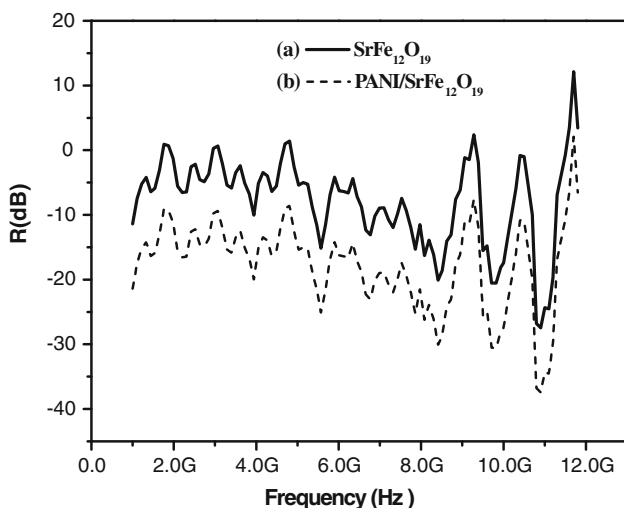
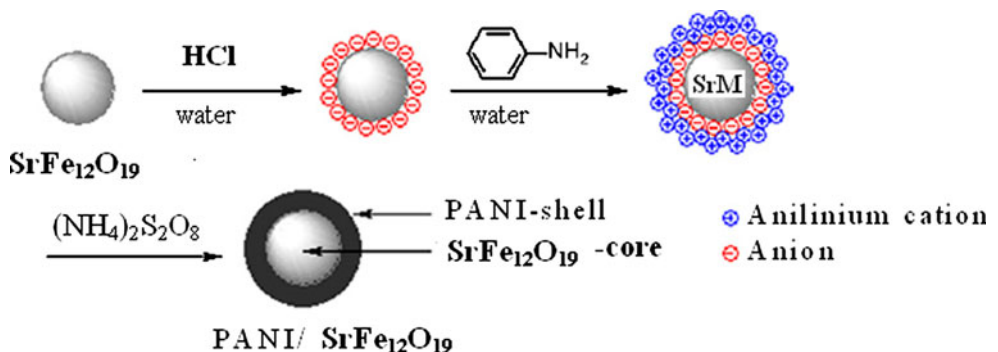


Fig. 7 The microwave absorption reflection loss of **a** SrFe₁₂O₁₉, **b** PANI/SrFe₁₂O₁₉

π -bond, in which the Fe³⁺ ions are the electron pair donors [18]. The polymerization mechanism for core–shell PANI/SrFe₁₂O₁₉ is shown in Fig. 6.

Microwave absorption

A high-frequency network analyzer (HP 8510C) was used to examine the reflectivities of the pure ferrites and the core–shell ferrites. Figure 7 shows the characteristic absorption of materials at frequencies between 1.0 and 12.0 GHz. It was found that the conductivity of PANI coated on the SrM dramatically affects the microwave absorption of materials. Composite specimens consisting of SrFe₁₂O₁₉, core–shell PANI/SrFe₁₂O₁₉ materials, and a thermal plastic resin demonstrated a microwave absorbing band-wide between 10.5 and 11.8 GHz, where reflections observed on a network analyzer lost from −27.3 to −37.4 dB.

Conclusion

A PANI/SrFe₁₂O₁₉ core–shell composite was successfully synthesized by the facile oxidative chemical polymerization

of aniline in the presence of SrFe₁₂O₁₉ particles. The core–shell structure of the PANI/SrFe₁₂O₁₉ composite was characterized by XRD, FT-IR, SEM, and TEM. The intrinsic magnetic hysteresis loop measurements revealed that the M_s and H_c increased with the polyaniline content. The conductivities of the core–shell materials increased with increasing amounts of PANI in the materials and with increasing temperature. The core–shell PANI/SrFe₁₂O₁₉–TPR materials have stronger absorption for microwave between 1.0 and 12.0 GHz than pure hexagonal ferrite, SrFe₁₂O₁₉–TPR. A nearly 40% band-width range of reflection loss peaks below −30 dB at frequencies between 8.0 and 11.8 GHz was observed in the core–shell PANI/SrFe₁₂O₁₉–TPR composite. The improvement in the adsorption performance may be attributed to the relative permittivity change induced by the exchange coupling interaction between the conducting polymer and the magnetic materials.

References

1. Mäkelä T, Pienimaa S, Taka T, Jussila S, Isotalo H (1997) *Synth Met* 85:1335
2. Kuwabata S, Masui S, Yoneyama H (1999) *Electrochim Acta* 44:4593
3. Kan JQ, Pan XH, Chen C (2004) *Biosens Bioelectron* 19:1635
4. Ahmad N, MacDiarmid AG (1996) *Synth Met* 78:103
5. Rose TL, Antonio SD, Jillson MH, Kron AB, Suresh R, Wang F (1997) *Synth Met* 85:1439
6. Gospodinova N, Terlemezyan L (1998) *Prog Polym Sci* 23:1443
7. Mathew RJ, Yang DL, Mattes BR (2002) *Macromolecules* 35: 7575
8. Yavuz O, Ram MK, Aldissi M, Poddar P, Hariharan D (2005) *J Mater Chem* 15:810
9. Zhang YY, Liu JL, Zhu YX, Shang Y, Yu M, Huang X (2009) *J Mater Sci* 44:3364. doi:[10.1007/s10853-009-3439-2](https://doi.org/10.1007/s10853-009-3439-2)
10. Wang JF, Ponton CB, Harris IR (2006) *J Magn Magn Mater* 298:122
11. Haijun Z, Zhichao L, Chengliang M, Xi Y, Liangying Z, Mingzhong W (2002) *Mater Sci Eng B* 96:289
12. Lee SP, Chen YJ, Ho CM, Chang CP, Hong YS (2007) *Mater Sci Eng B* 143:1
13. Ding H, Liu XM, Wan M, Fu SY (2008) *J Phys Chem B* 112: 9289

14. Jiang J, Li L, Xu F (2007) *J Phys Chem Solids* 68:1656
15. Huo J, Wang L, Yu H (2009) *J Mater Sci* 44:3917. doi:[10.1007/s10853-009-3561-1](https://doi.org/10.1007/s10853-009-3561-1)
16. Gorter EW (1950) *Nature (London)* 165:798
17. Sauzedde F, Elaissari A, Pichot C (1999) *Colloid Polym Sci* 277:846
18. Battle X, Labarta AJ, Phys D (2002) *Appl Phys* 35:15
19. Jiang J, Ai LH, Qin DB, Liu H, Li LC (2009) *Synth Met* 159:695